

# International Conference on Space Optics—ICSO 2018

Chania, Greece

9–12 October 2018

*Edited by Zoran Sodnik, Nikos Karafolas, and Bruno Cugny*



## *Cloud free line of sight prediction modeling for low earth orbit optical satellite networks*

*Nikolaos Lyras*

*Charilaos Kourogorgas*

*Athanasios Panagopoulos*



# Cloud Free Line of Sight Prediction for Low Earth Orbit Optical Satellite Networks

Nikolaos K. Lyras<sup>\*a</sup>, Charilaos I. Kourogiorgas<sup>a</sup>, Athanasios D. Panagopoulos<sup>a</sup>,  
<sup>a</sup>School of Electrical and Computer Engineering, National Technical University of Athens, Athens  
Greece

## ABSTRACT

In this paper, a methodology for the generation of cloud free line of site time series for low earth orbit optical satellite communication systems is presented. The proposed methodology is based on the synthesis of 3D cloud fields employing Integrated Liquid Water Content (ILWC) statistics. The methodology captures the temporal and spatial variability of cloud coverage and takes into account the varying elevation angle of the LEO optical link with each optical ground station (OGS) and the altitude of each OGS for the estimation of the CFLOS probability. The ILWC statistical parameters required for the CFLOS time series are taken from ERA Interim data base, European Centre for Medium-Range Weather Forecasts (ECMWF). Finally CFLOS numerical results are reported and some significant conclusions are drawn.

**Keywords:** FSO, LEO Satellite, cloud coverage, CFLOS, SDEs, ILWC, network, OGS.

## 1. INTRODUCTION

Free space optical (FSO) communications are considered as a promising prospect for non-geostationary satellite communication systems [1]-[3] and especially for LEO satellite applications. Compared to radio-frequency satellite systems, FSO technology has a great variety of advantages like capability for higher throughput, reduced mass, low energy consumption and improved security among others [3]. However, optical satellite communication systems are severely affected by weather conditions and mostly by clouds. The attenuation induced in the optical satellite signal due to clouds is so severe that the blockage of the link is considered [3], [4]. Therefore, an on/off channel with the occurrence of clouds is assumed [5]-[9]. In order to mitigate cloud coverage, optical ground stations site diversity technique is employed. For the reliable design of optical satellite communication systems, the Cloud-Free Line of Sight (CFLOS) probability should be accurately predicted for either single or multiple links (joint CFLOS statistics).

In the literature, approaches for the estimation of single and joint CFLOS probability mainly for GEO satellite communication systems are reported. In [8]-[10] single and joint CFLOS probability is estimated using cloud mask data, taking into account the spatial and temporal variability of clouds. Cloud mask data are derived from Earth observation from satellites like EUMETSAT system, MeteoSat, the NASA's Terra and Aqua satellites among others. Moreover in [2], [4]-[7] methodologies for the estimation of single and joint CFLOS statistics employing Integrated Liquid Water Content statistics are reported. In [4], the presented model captures the spatial and temporal correlation of clouds while the elevation angle of the satellite links and the altitude of the optical ground stations (very important in case of high altitude stations with altitude higher than the cloud top [4], [5]) are taken into account. In addition in [6], [7] the monthly and hemisphere variability of cloud coverage is examined and optimization algorithms for the OGS selection incorporating the before mentioned terms are proposed [7]. In [11] a methodology for the selection of the optimal OGS location for a LEO system is presented among others.

In this paper, a methodology for the estimation of CFLOS probability for a single OGS and a network of OGSs for a LEO satellite communication system is presented. The proposed methodology is based on the synthesis of 3D cloud fields employing stochastic differential equations (SDEs) using ILWC statistics as reported in [4]. The proposed methodology captures the variability of elevation angle for each OGS with the LEO satellite during the time for the estimation of CFLOS. Moreover, the temporal and spatial variability of cloud coverage and the altitude of the OGS are

also taken into account. The required inputs i.e. the statistical ILWC parameters are derived from ERA Interim database for each place of interest.

The remainder of the paper is structured as follows: In Section 2 the proposed methodology is reported. In Section 3 the CFLOS single and joint numerical results are presented using the proposed methodology. Finally Section 4 concludes the paper.

## 2. METHODOLOGY

In this Section the proposed methodology for the generation of single and joint CFLOS statistics for a single OGS and an OGS network (OGSN) respectively assuming a non-GEO satellite in our case LEO with time varying elevation angle is presented.

### 2.1 Elevation angles-System Definition

In this Subsection the estimation of the elevation angle for a single OGS communicating with a LEO satellite is reported. Employing AGI/STK tool kit [12], the sub satellite points of the LEO satellite are generated using a specific time resolution and for an orbital period. The time resolution of the sub satellite points is selected to be the same with the time resolution of CFLOS time series. When the LEO satellite is not in the visibility area of the OGS the elevation angle is considered zero. In addition, it is assumed that when the elevation angle is less than 20deg there is no connection with the satellite and again the elevation angle is set zero

For a single OGS the CFLOS statistics are computed given that the LEO satellite is within the visibility area of the station. For the site diversity scenario the joint CFLOS statistics are computed given that at least one station is in the visibility area. In the following Fig.1 the Probability Density Function of elevation angle (given that elevation angles are higher than 20deg) for a hypothetical OGS located in Heraklion, Crete, Greece given that the LEO satellite is in the visibility area is reported. Iridium LEO satellite is assumed (altitude: 779km, inclination angle 88.9 deg). Sub-satellite points have been generated for 1 year with 30sec temporal resolution.

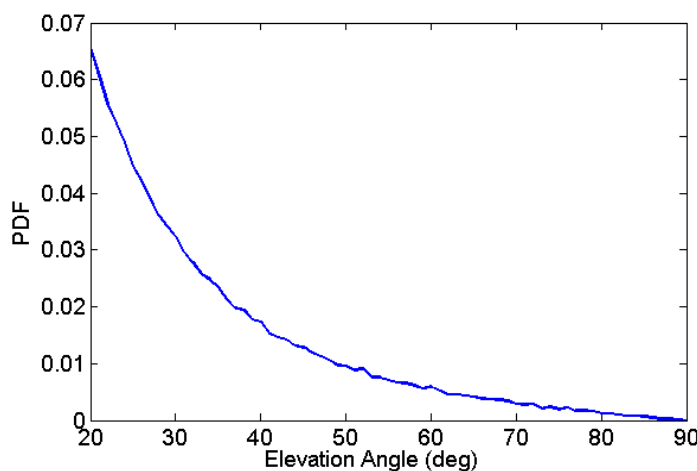


Figure 1 Elevation Angle PDF Heraklion-Iridium

### 2.2 CFLOS time series generator

To begin with, to capture the effect of clouds along the slant path depending on the elevation angle, the methodology reported in [4] will be used. Firstly for each station a 2-D ILWC map is generated. Each map consists of several ILWC grids with spatial resolution of 1km x 1km correlated in temporal and spatial domain. It is assumed that ILWC is constant for a grid of 1kmx1km. Since the ILWC map consists of several ILWC grids, the temporal and spatial correlation of ILWC along the slant path is taken into account. Such an ILWC map is reported in Figure 1. The ILWC map for a station can be exhibited as  $L_{map,OGS} = [L_1, L_2, \dots, L_n]$  where  $L_i$  are the ILWC grids along the slant path and  $n$  is the number of grids along the whole slant.

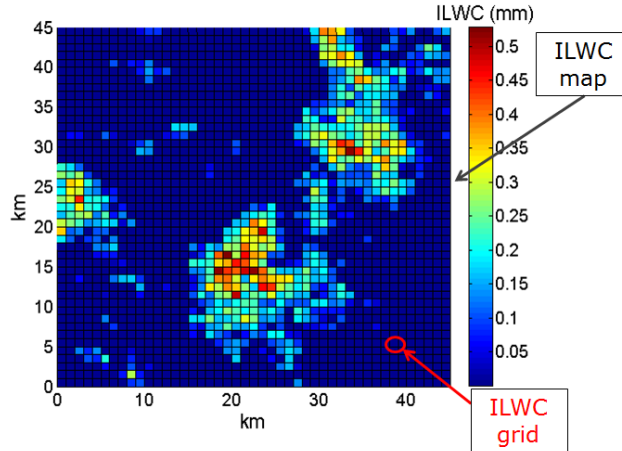


Figure 2 ILWC map Configuration

Now for a site diversity technique for each OGS a different ILWC map is generated. These maps are also correlated both in temporal and in spatial domain one to each other, i.e. the ILWC grids of OGS 1 are not only temporally and spatially correlated one to each other but also they are temporally and spatially correlated with the ILWC grids of OGS 2 etc. To this end the total ILWC field for a diversity scenario, where ILWC maps for different stations are incorporated can be expressed as  $L_{total\_field} = \begin{bmatrix} L_{map,OGS^1} & L_{map,OGS^2} & \dots & L_{map,OGS^k} \end{bmatrix}$ .

For the time series synthesis of ILWC the statistical parameters of  $\ln(L)$  i.e. the mean value ( $m$ ), the standard deviation ( $\sigma$ ) and the probability of cloud coverage ( $P_{clw}$ ) for each place of interest (OGS) are required and derived from meteorological databases. As adopted in ITU-R P.840 [13] and also studied in detail in [14] ILWC can be sufficiently described by lognormal distribution.

For synthesis of  $L_i$  multidimensional stochastic differential equations are employed according to the next expression [4] :

$$L_i(t) = \begin{cases} \exp \left[ Q^{-1} \left( \frac{1}{P_{CLW}} Q(G_i(t)) \right) \times \sigma + m \right] & G_i(t) \geq \alpha_{th} \\ 0 & G_i(t) \leq \alpha_{th} \end{cases} \quad (1)$$

where  $Q(\cdot)$  is the Gaussian Q-function. The statistical parameters can be considered constant along the slant path.  $\alpha_{th}$  is computed as  $\alpha_{th} = Q^{-1}(P_{CLW})$ .  $G_i(t)$  is the Gaussian process for the generation of each grid.  $G_i(t)$  can be defined as the superposition of two Gaussian processes [4] (2).

$$G_i(t) = \gamma_1 \cdot \mathbf{X}_{i,t}^1 + \gamma_2 \cdot \mathbf{X}_{i,t}^2, \quad (i = 1, \dots, n) \quad (2)$$

$\gamma_1, \gamma_2$  can be found in [15]. For the generation of each Gaussian process  $\mathbf{X}_{i,t}^k$  ( $k=1,2$ ) Stochastic Differential Equations are employed with the following solution [4]:

$$\mathbf{X}_{i,t}^k = e^{t \cdot \mathbf{B}^k} \cdot \mathbf{X}_0^k + e^{t \cdot \mathbf{B}^k} \cdot \int_0^t e^{-s \cdot \mathbf{B}^k} \cdot \mathbf{S}^k \cdot d\mathbf{W}_s, \quad (k=1, 2) \quad (3)$$

$\mathbf{W}(t)$  is the  $n$ -dimensional Wiener process. In  $\mathbf{B}^k$  matrix the dynamic parameters of the Gaussian processes of ILWC are incorporated [4], [15] while in matrix  $\mathbf{S}^k$  the spatial correlation of ILWC is incorporated according to [4].

In Figure 3 snapshots of 2-D ILWC maps correlated on spatial and temporal domain for a hypothetical OGS in Chania, Crete are presented. The left one is at time  $t=t_0$  while the right one is 60 min later. From these figures the temporal and spatial variability of clouds for a plane 50x50 km is pinpointed.

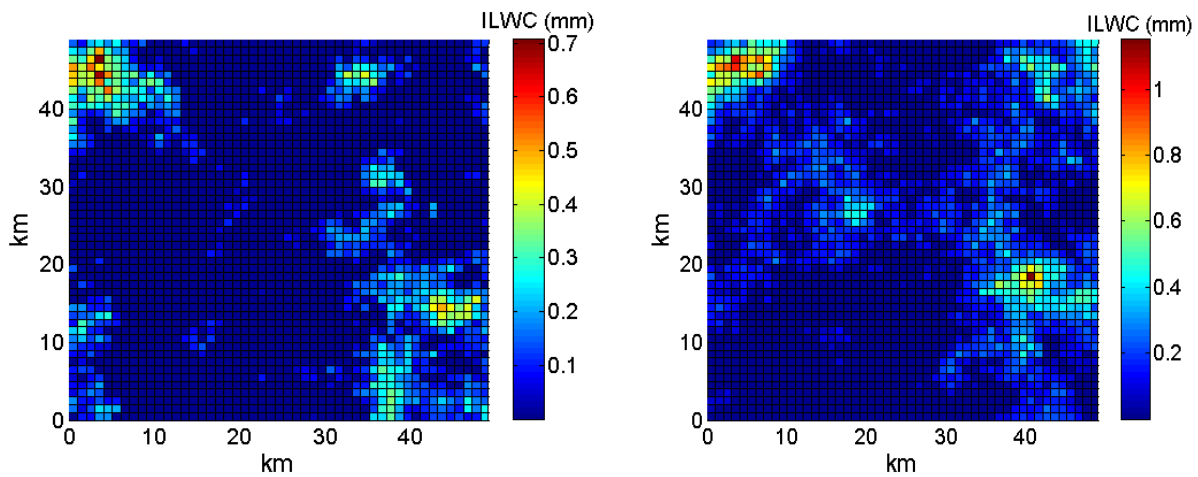


**Figure 3 Snapshots of ILWC 2-D maps correlated on spatial and temporal domain  
left  $t=t_0$ , right  $t=t_0+60\text{min}$**

To continue, in order to convert the 2-D maps to 3-D, the vertical extent of each ILWC grid (of each cloud) is defined employing the expression proposed in [16] for liquid water content depending on the ILWC and height. Solving the expression (4) of [16] the vertical extent for each cloud grid (1km x1km spatial resolution) of each map for each station is computed [4] [5]. It is assumed that the height is constant for the whole 1km x 1km grid. In expression (4) the height of cloud base is needed. If cloud base statistics for the OGS of interest are available can be used otherwise cloud base values can be derived from a proposed distribution in [16]. In Figure 4 the 2D cloud maps presented in Figure 3 are transformed in 3D. The color bar defines the vertical extent (the difference between the lowest and the highest point of the cloud). The first one is at time  $t=t_0$  while the second one is 60 min later.

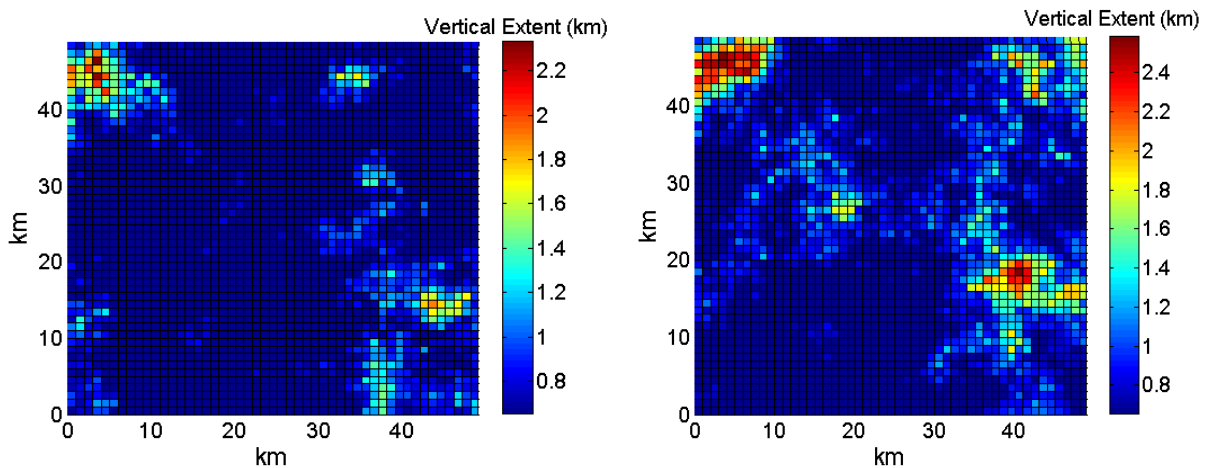


**Figure 4 Snapshots of 3D maps correlated on spatial and temporal domain-Vertical Extent  
left  $t=t_0$ , right  $t=t_0+60\text{min}$**

Since the vertical extent of each grid of each map is already known, the 3D configuration of clouds along the slant path is defined. Thus, CFLOS along the slant path can be estimated taking into account the elevation angle time series computed as reported in Section 2.1 for each OGS and the altitude of each OGS.

For each station it is assumed that if there is at least one cloud grid (grid with  $ILWC > 0$ ) with vertical extent that impairs the link along the slant path then the whole optical slant path is considered blocked. Thus, for each station concurrent CFLOS time series temporally and spatially correlated are generated. For an OGSN, if at least one station is not blocked by clouds, then the OGSN is considered free of clouds and the joint CFLOS statistics can be calculated.

The main steps of whole methodology are summarized bellow:

- Using AGI/STK tool the sub satellite points of LEO Satellite are computed
- Elevation angles for each OGS using the sub satellite points are computed
- ILWC maps (time series) for each OGS are generated using the proposed methodology
- Vertical extent for each ILWC grid is computed. 2-D ILWC maps are converted to 3D maps
- For each elevation angle CFLOS time series are computed.

### 3. NUMERICAL RESULTS

In this section the methodology reported before is used for the generation of single and joint CFLOS statistics for hypothetical OGSs in Greece. The numerical calculations have been implemented using MATLAB graphical environment. Firstly, in the following Figure, the capability of the ILWC space-time synthesizer to reproduce the first-order (exceedance probability) statistics of the theoretical curves from ITU-R databases (ECMWF ERA-40) [13] for a location is confirmed. It can be noticed that the CCDFs derived from the synthesized data and the ones from databases coincide.

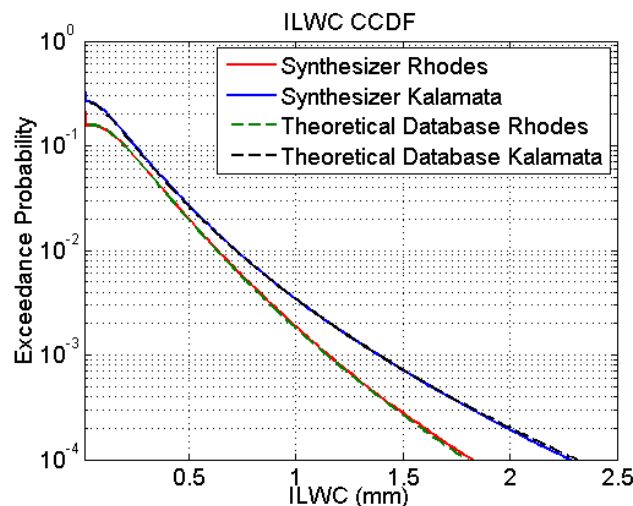


Figure 5 First order statistics validation of the ILWC synthesizer

In Figure 6 CFLOS is computed using the reported synthesizer for different elevation angles. A hypothetical link in Naxos is assumed while CFLOS is estimated for elevation angles from 20 to 90deg. Statistical parameters of ILWC are derived from ITU-R databases (ECMWF ERA-40) [13]. It can be easily pinpointed that for low elevation angles, CFLOS is lower while for elevation angles are more than 50 deg the CFLOS remains nearly constant. It comes from the fact that for low elevation angles the propagation path in the atmosphere increases and as a result the probability of a cloud present in the slant path increases.

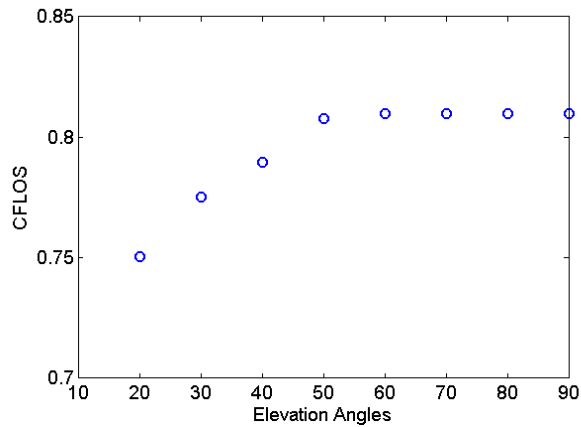


Figure 6 CFLOS vs Elevation Angle – Hypothetical OGS in Naxos

In the Figure 7 the hypothetical OGSs are depicted. Using as space segment the Iridium LEO satellite single OGS (Table 1) and joint CFLOS statistics are reported. The temporal resolution of both sub satellite points and the CFLOS time series is set as 30sec. As explained in Section 2.1 the single CFLOS statistics for each OGS are given that the LEO satellite is in the visibility area of the OGS. The joint CFLOS is computed for time instants that the LEO satellite is in the visibility area for at least one OGS.

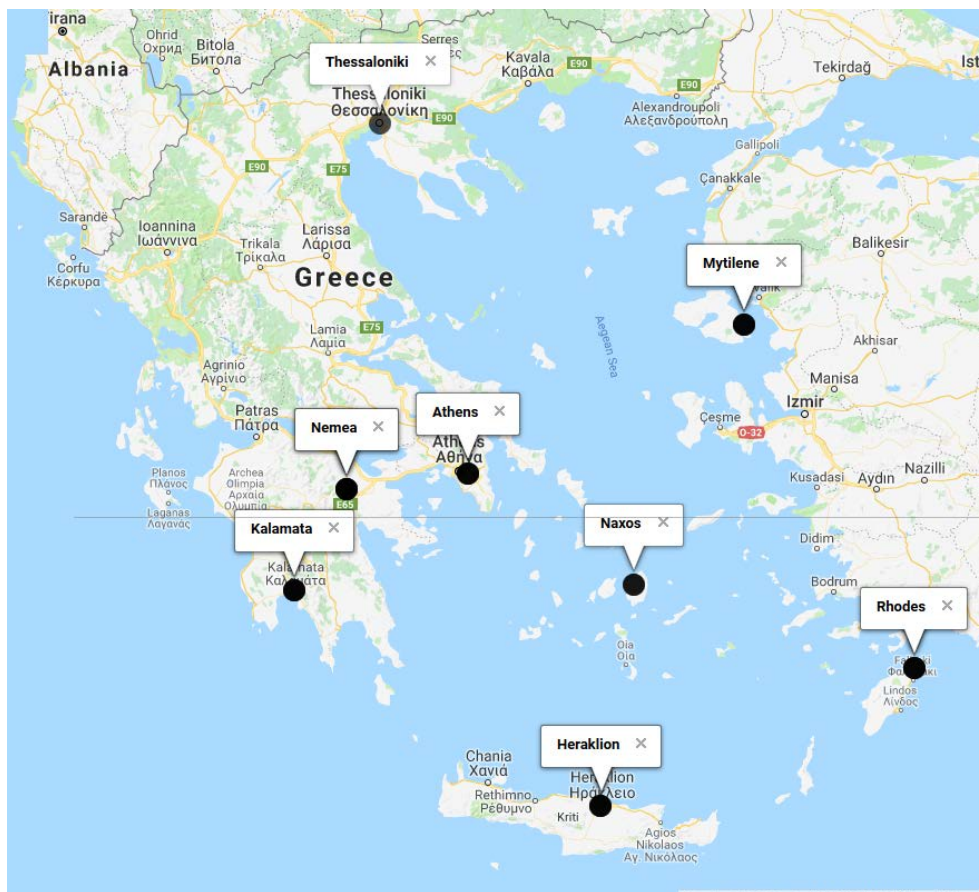


Figure 7 Hypothetical OGS Network

For each station the PDF of elevation angles is computed as reported in Section 2.1 and in Table 1 CFLOS is computed for each hypothetical OGS. Now for the estimation of CFLOS the mean statistical parameters of ILWC are derived from ERA Interim database (ECMWF) for years from 2000 until 2016 (different database from the one used for the results in Figure 6).

**Table 1 Single OGS CFLOS Probability**

Location	Latitude (deg)	Longitude (deg)	Altitude (m)	Min-Max Elev. Angle(deg)	CFLOS (%)
Nemea	37.84	22.62	440	20-89.4	55.6
City of Heraklion, Crete	35.33	25.13	400	20-89.86	69.1
Athens	37.96	23.82	500	20-89.6	62.2
Kalamata	37.05	22.102	400	20-89.6	61.4
City of Rhodes,	36.43	28.22	300	20-89.4	71.7
Mytilene, Lesvos	39.11	26.54	420	20-89.5	64.6
Thessaloniki	40.64	22.95	430	20-89.8	53.5
Naxos	37.09	25.46	500	20-89.3	68.3

Finally assuming that the above stations forming a regional OGSN the joint CFLOS is estimated as 91.32%.

#### 4. CONCLUSIONS AND FUTURE WORK

To conclude in this paper a space time synthesizer for the estimation of CFLOS for a single link or a spatial diversity scenario assuming non-GEO satellites and especially a LEO satellite as space segment based on the 3D synthesis of cloud fields is reported. The proposed synthesizer incorporates the spatial and temporal correlation of ILWC and takes into account the varying elevation angle of a LEO satellite among others. The proposed algorithm is employed for the generation of numerical results using a hypothetical OGS network in Greece and a LEO satellite.

Since high altitude stations are of prominent importance for optical satellite communications systems, studies about the height of cloud base and the vertical extent of clouds especially for high altitude stations can be proved beneficial. Some analysis has already been conducted [16] however dedicated studies for high altitude locations can improve the accuracy of CFLOS prediction.

#### REFERENCES

- [1] Toyoshima, M. *et al.*, "Trends in satellite communications and the role of optical free-space communications [Invited]," *J. Opt. Netw.* 4, 300-311 (2005).
- [2] Kourogorgas, C. I., *et al.*, "Capacity Statistics Evaluation for Next Generation Broadband MEO Satellite Systems," in *IEEE Transactions on Aerospace and Electronic Systems*, vol. 53, no. 5, pp. 2344-2358, Oct. 2017.
- [3] Kaushal, H., Kaddoum G., "Optical Communication in Space: Challenges and Mitigation Techniques," in *IEEE Comm. Surv. & Tut.*, no.99, pp.1-1.
- [4] Lyras, N.K., Kourogorgas, C.I. and Panagopoulos, A.D., "Cloud Attenuation Statistics Prediction From Ka-Band to Optical Frequencies: Integrated Liquid Water Content Field Synthesizer," in *IEEE Transactions on Antennas and Propagation*, vol. 65, no. 1, pp. 319-328, Jan. 2017.
- [5] N. K. Lyras, C. I. Kourogorgas and A. D. Panagopoulos, "Cloud Free Line of Sight Prediction Modeling for Optical Satellite Communication Networks," in *IEEE Communications Letters*, vol. 21, no. 7, pp. 1537-1540, July 2017.
- [6] Lyras, N.K., *et al.*, "Monthly and Seasonal CFLOS Statistics for Optical GEO Feeder Links Design" in *WISATS*, 2017, Oxford.

- [7] Lyras, N. K. , *et.al.*, ""Optimum Monthly Based Selection of Ground Stations for Optical Satellite Networks," in IEEE Communications Letters, vol. 22, no. 6, pp. 1192-1195, June 2018.
- [8] Fuchs, C., Moll, F., "Ground station network optimization for space-to ground optical communication links," in IEEE/OSA J. of Opt. Comm. and Net., vol. 7, no. 12, pp. 1148-1159, Dec.2015
- [9] Sanchez, Net, M. *et al.*, "Approximation Methods for Estimating the Availability of Optical Ground Networks" J. Opt. Com. Net. 8, 800-812 2016
- [10]Poulenard, S., Crosnier, M., and Rissons, A. , "Ground segment design for broadband geostationary satellite with optical feeder link," J. Opt. Commun. Netw., vol. 7, no. 4, pp. 325–336, 2015.
- [11]I. del Portillo, et al. "Optimal location of optical ground stations to serve LEO Spacecraft" 2017 IEEE Aerospace Conf. Big Sky, MT, 2017, pp. 1-16.
- [12]"AGI STK." [Online]. Available: <https://www.agi.com/products/byproduct-type/applications/stk/>
- [13]ITU-R Recommendation P.840-6, "Attenuation due to clouds and fog." Geneva, Switzerland, 2013.
- [14]Jeannin, N., *et al.*, "Statistical Distribution of Integrated Liquid Water and Water Vapor Content From Meteorological Reanalysis", IEEE Transactions on Antennas and Propagation, vol. 56, pp. 3350-3355, 2008.
- [15]ITU-R Recommendation P.1853-1 "Tropospheric attenuation time series synthesis," ITU-R P.1853-1, vol. ITU-R P Series Recommendations Radio wave Propagation, 2012
- [16]Luini, L., Capsoni, C. , "Modeling High-Resolution 3-D Cloud Fields for Earth-Space Communication Systems," IEEE Transactions on Antennas and Propagation, vol.62, no.10, pp.5190,5199, Oct. 2014